THE JOURNAL OF PHYSICAL CHEMISTRY B

Article

pubs.acs.org/JPCB

Evidence for the Interactions Occurring Between Ionic Liquids and Tetraethylene Glycol in Binary Mixtures and Aqueous Biphasic Systems

Luciana I. N. Tomé,[†] Jorge F. B. Pereira,[†,‡] Robin D. Rogers,[‡] Mara G. Freire,[†] José R. B. Gomes,[†] and João A. P. Coutinho*[,†]

[†]Departamento de Química, CICECO, Universidade de Aveiro, 3810-193 Aveiro, Portugal

[‡]Center for Green Manufacturing and Department of Chemistry, The University of Alabama, Tuscaloosa, Alabama 35487, United States

Supporting Information

ABSTRACT: The well-recognized advantageous properties of poly(ethylene glycol)s (PEGs) and ionic liquids (ILs) in the context of an increasing demand for safe and efficient biotechnological processes has led to a growing interest in the study of their combinations for a wide range of procedures within the framework of green chemistry. Recently, one of the most promising and attractive applications has been the novel IL/polymer-based aqueous biphasic systems (ABS) for the extraction and purification of biomolecules. There still lacks, however, a comprehensive picture of the molecular phenomena that control the phase behavior of these systems. In order to further delve into the interactions that govern the mutual solubilities between ILs and PEGs and the formation of PEG/IL-based ABS, ^{1}H NMR spectroscopy in combination with classical molecular dynamics (MD) simulations performed for binary mixtures of tetraethylene glycol (TEG) and 1-alkyl-3-methylimidazolium-chloride-based ILs and for the corresponding ternary TEG/IL/water solutions, at T = 298.15 K, were employed in this work. The results of the simulations show that the mutual solubilities of the ILs and TEG are mainly governed by the hydrogen bonds established between the chloride anion and the −OH group of the polymer in the binary systems. Additionally, the formation of IL/PEG-based ABS is shown to be controlled by a competition between water and chloride for the interactions with the hydroxyl group of TEG.

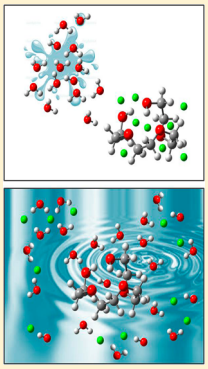

1. INTRODUCTION

The search for efficient and safe approaches to improve the standards of industrial and biotechnological procedures has led to a growing interest in the development of novel materials, chemical media, and technologies. Poly(ethylene glycol)s (PEGs) are one of the most widely used classes of polymers in the chemical and life-sciences industries.[1] Some of their most attractive properties are related to their biodegradability, low toxicity, low volatility, low melting points, enhanced water solubility, and low cost[2] and make them convenient for a variety of important applications including drug delivery, protein partitioning, polymer surfactants, polymer electrolytes, viscosity modifications, and separation or purification techniques, such as aqueous biphasic systems, among others.[3−12]

Because of the biotechnological and industrial relevance of PEGs, a large number of experimental and theoretical investigations of their structure−property relationships[13−15] and of the behavior and structure of their mixtures with other solvents,[16,17] especially of their aqueous solutions,[18−22] has been undertaken. Recently, in the face of the popularity and well-recognized advantageous characteristics of ionic liquids (ILs),[23−27] combinations of ILs and PEGs have been proposed for different uses within the framework of green chemistry.[28−35] In this context, the exploration of the novel polymer/IL-based aqueous biphasic systems (ABS) in the domains of extraction and purification technologies has earned special attention and seems to be particularly promising.[31,32,36−39]

For the improvement and optimization of the existing applications and for the development of new ones, a detailed knowledge of the behavior of both binary mixtures of ILs and PEGs and ternary aqueous solutions of these compounds, as well as of their underlying molecular mechanisms, is essential. In this respect, experimental and theoretical data for these systems are yet scarce,[31,32,34,36,40] and despite some of the insight already acquired on the interactions that control the phase behavior of PEG/IL mixtures[34] and of PEG/IL-based ABS,[31,32,36,40] a clear and well-supported molecular picture of the basic molecular phenomena is still lacking. Recently, we have demonstrated that some IL/PEG/water systems are of Type 0 and provided novel evidence for a "washing-out" mechanism behind the formation of PEG/IL-based ABS.[40] In order to further delve into the molecular interactions that govern the solubility of ILs and PEGs and the formation of PEG/IL-based ABS, aqueous solutions of the IL 1-butyl-3-methylimidazolium chloride, [C_4mim]Cl, and the polymer poly(ethylene glycol) 200 (PEG-200) were studied in this work

Received: February 18, 2014
Revised: April 9, 2014
Published: April 10, 2014

using ^{1}H NMR spectroscopy. PEG-200 is a mixture of isomeric polymers which have 4 EO units and an average molecular mass of 200. The most abundant component is tetraethylene glycol, which has a molecular weight of 194. To support the experimental results and achieve a deeper understanding of these systems, classical molecular dynamics (MD) simulations were performed for binary mixtures of tetraethylene glycol (TEG) and 1-alkyl-3-methylimidazolium-based ILs (1,3-dimethylimidazolium chloride, [C_1mim]Cl, 1-ethyl-3-methylimidazolium chloride, [C_2mim]Cl, [C_4mim]Cl, and 1-hexyl-3-methylimidazolium chloride, [C_6mim]Cl) (Figure 1), and for the corresponding ternary aqueous solutions constituted by TEG/IL/water at T = 298.15 K. TEG was here used as a model PEG since, unlike high molecular weight PEGs, its moderate size enables a reliable equilibration with MD methods in a reasonable amount of computer time. In addition, this glycol has important applications, for instance, as a drying agent for natural gas, humectant, solvent, and in the manufacture of vinyl plasticizers.[41] Imidazolium as an IL ion has been the most appealing and most frequently considered, and is known for its nondenaturing nature, low toxicity, and reduced water pollution risk, when containing a short alkyl side chain length.[42,43] In this work, we evaluated the interactions between imidazolium chloride ionic liquids with PEGs, in binary systems or in the presence of water, and the effect of the length of the cation alkyl side chain on these interactions.

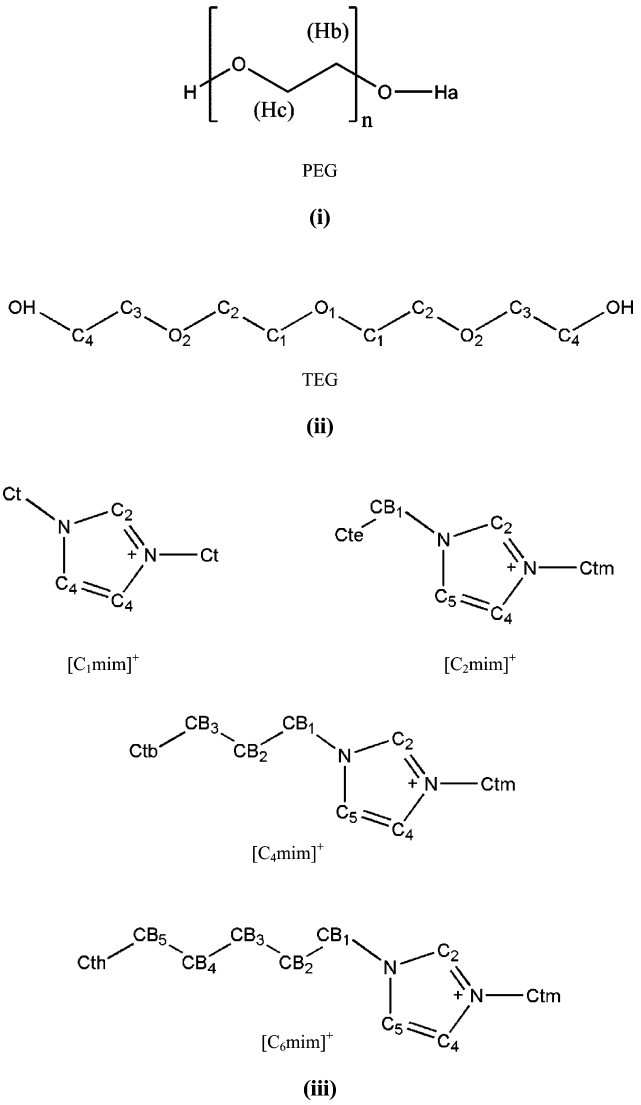

Figure 1. Structure and atom labeling of (i) PEG, (ii) TEG, and of the (iii) IL cations studied in this work. Ctm, Cte, Ctb, and Cth stand, respectively, for the terminal carbon atoms of the methyl, ethyl, butyl, and the hexyl side chains of the IL cation, while CB_x (x = 1, 2, 3, 4, 5) is used to denote the other carbon atoms of the alkyl chains. Hydrogen atoms of the molecules, omitted for clarity, are labeled with the number of the carbon atoms to which they are attached.

MD simulation has proved to be a valuable tool for the investigation of (bio)chemical systems[44−49] and has been previously successfully used to characterize the interactions established in aqueous saline solutions of amino acids,[50,51] in aqueous solutions of imidazolium-based ILs in the presence of salts,[52] and in IL/amino acid/water mixtures,[53] and to provide insight into the mechanisms underlying the phase behavior presented by some ternary IL/PEG/water systems.[40] The MD approach was also considered in the understanding of the fundamental chemistry of ILs and of their mixtures with different compounds,[54−57] and in structural studies of PEGs and of their aqueous solutions.[15,49,58−61]

2. NMR EXPERIMENTAL SECTION

For the NMR studies, IL [C_4mim]Cl and PEG-200 were employed. The IL was supplied by Iolitec with a mass fraction purity of 99%, and PEG-200 was acquired from Fluka. To reduce the water content and volatile compounds to negligible values, both the IL and PEG were dried under reduced pressure (p < 1 Pa) at ca. 333 K using constant stirring, for a minimum of 48 h. The deuterium oxide and the 3-(trimethylsilyl)-propionic-2,2,3,3-d_4 acid sodium salt (TSP) were from Aldrich with, respectively, >99.96% D atoms and >98% D atoms. The water used for the preparation of the aqueous solutions was double-distilled, passed by a reverse osmosis system, and further treated with a Milli-Q plus 185 water purification apparatus. It had a resistivity of 18.2 MΩ cm, a total organics content smaller than 5 $\mu g \cdot dm^{-3}$, and was free of particles greater than 0.22 μm.

For the ^{1}H NMR measurements, three sets of experiments were performed: one for different [C_4mim]Cl molalities, one for different PEG-200 molalities, and another one for varying the water concentration. For the first two sets, a solution of [C_4mim]Cl (or PEG-200) at approximately 1 $mol \cdot kg^{-1}$ in D_2O, using TSP as a reference, was prepared gravimetrically with an associated uncertainty of $\pm 10^{-4}$ g. The PEG-200 (or [C_4mim]-Cl) solutions were prepared gravimetrically in the D_2O-[C_4mim]Cl (or PEG-200) initial solution with PEG-200 (or [C_4mim]Cl) concentration ranging from 0 to 1 $mol \cdot kg^{-1}$. The ^{1}H NMR spectra were obtained for the initial D_2O-[C_4mim]Cl (or D_2O-PEG-200) solution and for the different ternary mixtures using a Bruker Avance 300 spectrometer operating at 300.13 MHz, with D_2O as solvent and TSP as internal reference. For the third set of experiments, a solution of [C_4mim]Cl at approximately 1 $mol \cdot kg^{-1}$ in PEG-200 was prepared gravimetrically with an associated uncertainty of $\pm 10^{-4}$ g. The aqueous solutions were prepared gravimetrically in the [C_4mim]Cl-PEG200 initial solution with water molalities ranging from 0 to 5 $mol \cdot kg^{-1}$. The ^{1}H NMR spectra were obtained for the initial PEG-IL solution and for the different ternary mixtures placed in NMR spectroscopy tubes containing sealed reference capillaries with D_2O and TSP as the internal reference, and at 298 K. The ^{1}H NMR measurements were

dx.doi.org/10.1021/jp501718w | J. Phys. Chem. B 2014, 118, 4615−4629

performed on a Bruker Avance 300 spectrometer operating at 300.13 MHz.

For each set, the ^{1}H NMR chemical shift deviations were defined according to eqs 1, 2, and 3, respectively:

$$\Delta\delta_H = \delta_H(\text{IL} + \text{PEG-200} + D_2O) - \delta_H(\text{IL} + D_2O) \quad (1)$$

$$\Delta\delta_H = \delta_H(\text{IL} + \text{PEG-200} + D_2O) - \delta_H(\text{PEG-200} + D_2O) \quad (2)$$

$$\Delta\delta_H = \delta_H(\text{IL} + \text{PEG-200} + H_2O) - \delta_H(\text{IL} + \text{PEG-200}) \quad (3)$$

where δ_H(IL + PEG-200 + D_2O) is the ^{1}H NMR chemical shift of the protons in the (IL + PEG-200 + D_2O) solutions, δ_H(IL + PEG-200 + H_2O) is the ^{1}H NMR chemical shift of the protons in the (IL + PEG-200) aqueous solutions, and δ_H(IL + D_2O), δ_H(PEG-200 + D_2O), and δ_H(IL + PEG-200) are the ^{1}H NMR chemical shifts of the protons in the absence of PEG-200, IL, or water, respectively.

3. COMPUTATIONAL METHODS

MD calculations were performed for TEG/IL binary and TEG/IL/water ternary mixtures, for four imidazolium-based ILs at concentrations (50 wt % of TEG, 30 wt % of IL, and 20 wt % of water) approximately reproducing the monophasic region of the experimental phase diagrams obtained with PEGs.[34,40] The simulations were carried out using the isothermal−isobaric *NpT* (T = 298.15 K and p = 1 bar) ensemble and the GROMACS 4.07 molecular dynamics package.[62] The equations of motion were integrated with the Verlet-Leapfrog algorithm[63] and a time step of 2 fs. The Nosé−Hoover thermostat[64,65] was used to fix the temperature, while the Parrinello−Rahman barostat[66] was employed to fix the pressure. Starting configurations were generated in cubic boxes with lateral dimensions of 45 Å, and periodic boundary conditions were applied in three dimensions. The systems were prepared by randomly placing all species in the simulation box. For the calculations of the ternary solutions, 60 [C_1mim](/[C_2mim]/[C_4mim]/[C_6mim])Cl ion pairs, 80 TEG molecules, and 380 water molecules were incorporated in each box, while for the binary systems, 90 [C_1mim](/[C_2mim]/[C_4mim]/[C_6mim])Cl ion pairs and 120 TEG molecules were included. A 10 000 step energy minimization was performed followed by two simulations, the first one with 50 000 steps for equilibration and the final one with 10 000 000 steps (20 ns) for production. After equilibration, the values of the box volume ranged between 50.0 and 45.1 nm^3 (ternary systems) and between 52.8 and 65.4 nm^3 (binary systems), depending on the IL considered. Equilibration was checked by ensuring that all observables (including the RDFs) fluctuated around their equilibrium values during the production state.

The intermolecular interaction energy between pairs of neighboring atoms was calculated using the Lennard-Jones potential to describe dispersion/repulsion forces, and the point-charge Coulomb potential was used for electrostatic interactions. Long-range electrostatic interactions were accounted for using the particle-mesh Ewald method[67] with a cutoff of 1.0 nm for the real-space part of the interactions. A cutoff radius of 1.2 nm was used for the Lennard-Jones potential, and long-range dispersion corrections were added to both energy and pressure. All bond lengths were held rigid using the LINCS constraint algorithm,[68] while angle bending was modeled by a harmonic potential, and dihedral torsion was described (where appropriate) by a Ryckaert-Bellemans function.

It is well recognized that the choice of the force field to be used in MD simulations is a crucial aspect since it often has repercussions on the accuracy of the results obtained.[48,69−72] For ILs and PEGs, in particular, the formulation of potentials capable of representing their energetics and structure has been a nontrivial and challenging subject. In the case of ILs, there have been difficulties associated with the fact that these solvents are neither simple molecular fluids nor common (high-melting) salts but exhibit complex interactions between their constituting ions and, however, show a paucity of experimental data published for the very large number of possible ILs.[69−72] Despite such problems, significant progress has been made in the application of MD methods to IL systems, and force field parameters have already been developed and validated for a large number of cations and anions, yielding reliable results.[69−72]

Potentials available in the literature were taken for all the species considered in the simulations.[73−76] As far as PEGs are concerned, the main issues are related to the highly complex inter- and intramolecular interactions and to their considerable conformational flexibility.[49,77] Considerable efforts have been made toward the development of potentials that can accurately account for such phenomena. Several force fields have been parametrized and revised with appropriate adjustments, and quality potentials exist for PEGs, including ethylene glycol, triethylene glycol, tetraethylene glycol, and poly(ethylene glycol)s, which can reproduce structural and thermodynamic properties over a wide range of systems and conditions.[15,49,58,60,61,77,78] In this work, the potential used for TEG is based on the OPLS all-atom potential from Jorgensen and Tirado-Rives[73] for diethylene glycol using the ESP charges taken from the Automatic Topology Builder Web site[79] calculated for the B3LYP/6-31G* optimized structure of 3,6,9,12-tetraoxatetradecane-1,14-diol. To test and validate the force field selected for TEG, preliminary MD calculations of pure TEG and of binary aqueous solutions (the rigid SPC/E model[74] was used for the water molecules) of the glycol were carried out, under varied simulation conditions. The values of the density of pure TEG (1124.17 kg m^{-3}) and of the aqueous solutions of TEG as a function of the polymer concentration (Table S1, Supporting Information) calculated from the MD results are in good agreement with the experimental literature data[17,80−82] (maximum deviation 1.4%) (Figure S1, Supporting Information), affording further consistency to our results.

The all-atom force field parameters for the IL cations were obtained from the work of Cadena and Maginn[75] and for the anion from the OPLS all-atom potential.[76] The force field selected in this work for the cations[75] has been successfully parametrized and tested, providing accurate descriptions of ILs and their mixtures.[52−54,83] The atomic charges for the cations were recalculated in this work with the CHelpG scheme using an optimized geometry for the [C_1mim]$^+$/[C_2mim]$^+$/[C_4mim]$^+$/[C_6mim]$^+$ cations in the gas phase. The calculations considered the B3LYP/6-311+G(d) approach as included in the Gaussian 09 code,[84] i.e., using the same computational strategy employed by Morrow and Maginn for the [C_4mim]-[PF_6] ionic liquid.[85] The full set of atomic charges is supplied as Supporting Information (Tables S2−S6).

In order to provide more consistency and support to the molecular interpretations given in this work, additional MD calculations were performed for TEG/water and TEG/

dx.doi.org/10.1021/jp501718w | J. Phys. Chem. B 2014, 118, 4615−4629

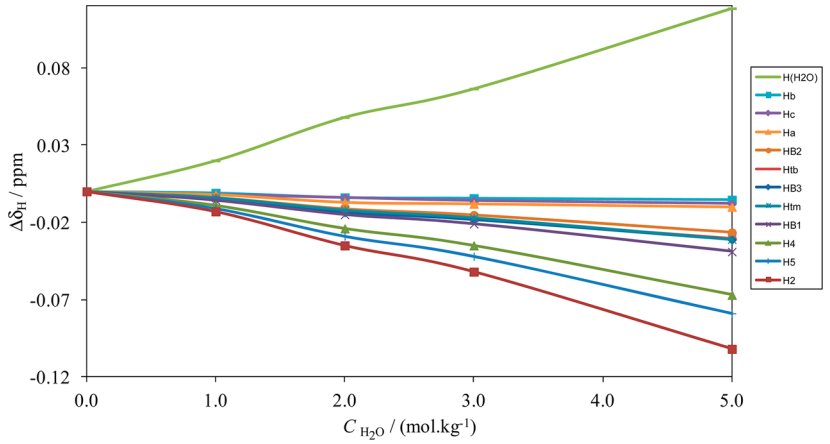

Figure 2. ^{1}H NMR chemical shift deviations in water, PEG-200, and [C_4mim]Cl relative to that of the initial PEG/IL binary mixture as a function of the water molality.

Na_2SO_4/water systems, following the same procedure and simulation conditions described above. In the first case, 80 TEG and 380 water molecules were incorporated in the simulation box. For the aqueous saline solutions of TEG, 80 TEG, 380 water molecules, 60 SO_4^{2-} anions, and 120 Na^+ cations were included in the simulation box. The OPLS all-atom potential was used for the sodium cation,[86] and the force field parameters of the second model proposed by Cannon et al.[87] were used for sulfate.

4. RESULTS AND DISCUSSION

4.1. NMR Spectroscopy. The chemical structure and atom numbering for the IL studied and for PEG-200 are depicted in Figure 1. The compositions of the experimental phase diagram of the ABS composed of PEG-200 and [C_4mim]Cl at which the ^{1}H NMR experiments were performed are provided in Figure S2 and Table S7 (Supporting Information). The results obtained for the three sets of ^{1}H NMR experiments performed are displayed in Figure 2 and Figures S3 and S4 (Supporting Information), which show the ^{1}H NMR chemical shift deviations for the PEG-200 and [C_4mim]Cl solutions, as a function of water, PEG-200, and IL concentration, respectively.

Although the molecular interpretation of the phase demixing in typical ABS based on PEG and inorganic salts has generated much debate over the years, it is currently almost consensual that in most cases the main driving force that controls the ABS formation is the creation of hydration complexes of the ions that induce the polymer salting-out.[88−90] The current understanding of the mechanisms behind the formation of the novel PEG/IL ABS is far more incipient. Despite some insight derived from the few recent experimental[31,32,36−40] and theoretical[40] studies, there still lacks a clear and comprehensive picture of the underlying molecular phenomena. It has been previously shown by us[40] using experimental and theoretical studies that the main interactions controlling the mutual solubilities of [C_4mim]Cl and PEG are the hydrogen bondings occurring between Cl^- and the −OH groups of PEG and that hydrogen bonds are also established between the polymer and the IL cation, at the level of the hydrogen atoms of the imidazolium ring. Furthermore, MD calculations have shown these interactions to be destroyed when water is introduced in the system and replaced by more favorable and stronger water−IL interactions, in what we labeled a "washing-out" phenomenon.[40]

The ^{1}H NMR spectroscopic data obtained in this work for the first two sets of experiments, where the IL (or PEG-200) concentration was varied, confirm that favorable interactions (positive deviations) between the imidazolium protons of the [C_4mim]$^+$ cation and PEG-200 (Figure S3, Supporting Information) and between the hydrogen atoms of the glycol and the IL (Figure S4, Supporting Information) are present and that these become more pronounced with the increase in the concentration of PEG-200 or [C_4mim]Cl, respectively, or, in other words, with the decrease of D_2O molality. However, the interactions occurring between the hydrogen atoms of the alkyl chain of the IL cation and PEG-200 are less favorable (negative deviations), and their strength decreases with the concentration of the glycol (Figure S3, Supporting Information), showing that these dispersive interactions do not have a dominant effect. Further evidence for this behavior can be obtained from the results displayed in Figure 2 for the chemical shift deviations between water and the solutes in the aqueous solutions, as a function of water molality, derived from the third set of NMR experiments performed. Actually, deviations which become more negative with water concentration are observed for all the [C_4mim]Cl protons considered, indicating that all the glycol−IL cation interactions become less favorable with the increase in water molality. The most important deviations are found for the H2, H4, and H5 atoms of the imidazolium cation ring, and no significant deviations are observed for the Ha, Hb, and Hc protons of PEG-200. Conversely, the water−water interactions become more favorable as the water content increases.

The picture that emerges from the NMR spectroscopic data is that the interactions of PEG with the IL become less favorable with increasing water content in the system, suggesting a preferential solvation of both the cation and the anion of the IL. These results are consistent with the "washing-out" mechanism previously proposed as the main mechanism controlling the formation of PEG/IL-based ABS.[40]

4.2. Molecular Dynamics Simulation. To further delve into the mechanisms governing the behavior of PEG/IL-based ABS, radial distribution functions (RDFs) were calculated from the MD simulations of TEG and ILs binary systems and of the corresponding ternary aqueous solutions. The RDFs provide a quantitative description of enhancement (values larger than 1) or depletion (values smaller than 1) of densities of species around a selected moiety, helping to understand the dominant intermolecular interactions present. They are presented below

for binary and ternary systems. The compositions of the experimental phase diagram of the ABS composed of PEG-200 and [C_4mim]Cl at which the MD simulations were performed are provided in Figure S2 and Table S7 (Supporting Information). MD simulation results obtained for the [C_4mim]Cl/water binary and [C_4mim]Cl/TEG/water ternary systems at different compositions of the mixture in the biphasic region of the [C_4mim]Cl/PEG1500/water experimental phase diagram[40] (Table S8, Supporting Information) are similar to those obtained and discussed in this work.

4.2.1. Binary Systems. To identify the most important interactions governing the mutual solubilities between TEG and ILs and to evaluate the role of the length of the alkyl side chain of the IL cation, we analyzed a large number of RDFs for the cation and anion of each IL around the distinct moieties of the glycol. In Figures 3 and 4, we present the most relevant

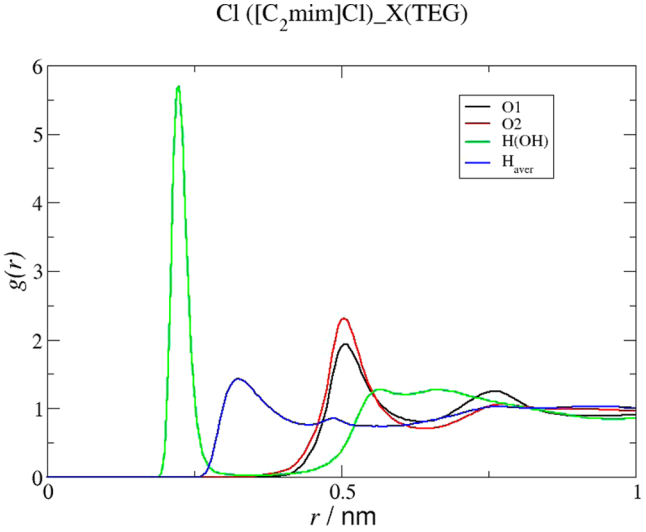

Figure 3. Radial distribution functions between the anion of [C_2mim]Cl and different regions of TEG. H_{aver} refers to the averaged interaction between the chloride anion and H1, H2, H3, and H4 atoms of TEG.

RDFs for the interactions between different molecular regions of TEG and the [C_2mim]Cl constituting ions. The first noticeable result is that the most significant interactions of TEG are established with the IL anion, as revealed by the RDF peaks displayed in Figure 3, which are globally more intense and occur for shorter distances than those corresponding to the association of TEG to the IL cation. Actually, Figure 3 shows a first very intense peak referring to the contact between the anion and TEG, more specifically, for the pair Cl^-···H(OH) (please refer to Figure 1 for atom labeling), which indicates the presence of substantial Cl^- structuring around the hydroxyl group, followed by a peak with smaller, yet also significant, intensity corresponding to the binding of Cl^- to the H atoms of the TEG alkyl chain. The strength of these interactions decrease in the order Cl^-···H3(TEG)>Cl^-···H2(TEG) ≈ Cl^-···H1(TEG)>Cl^-···H4(TEG) (Figure S5, Supporting Information), as suggested by the relative intensity of the RDF peaks. The RDFs of Figure 3 show also rather intense peaks for the association of the chloride to the ether oxygen atoms of TEG, but their distant positions suggest that this interaction is the result of the interactions with the hydrogen atoms, as expected from the negative charges of the oxygen atoms.

The IL cation−TEG interactions are much weaker than those involving the anion. For the cation, the strongest interactions are established at the level of the hydrogen atoms of the imidazolium ring. As shown in Figure 4, panels a and b, the peaks corresponding to the binding of H2(cation), the most acidic proton of the cation, to O1(TEG) and H4(cation) to O(OH)(TEG) are relatively intense and occur at very short distances, suggesting the presence of H-bonding between the IL cation and TEG. Because H2 is more acidic than H4, the interactions established between H2 and the TEG oxygen atoms are likely to be stronger than those occurring between H4 and the oxygen atoms of TEG. Remember that the potential used for the IL cation considers slightly more positive charge, smaller sigma and larger epsilon values in H2 than in H4 and H5, and therefore, the H4−O interaction peaks appear at longer distances than the H2−O ones. The interaction patterns observed for H4(cation) are similar to those observed for H5(cation). It is worth noticing that the H2 and H4 atoms of $[C_2mim]^+$ and the chloride ion are located at similar distances around TEG, as indicated by the relative positions of the H2(cation)···O1(TEG), H4(cation)···O(OH)(TEG), and Cl^-···H(OH)(TEG) peaks. These results are in agreement with data obtained from thermodynamic and spectroscopic studies of mixtures of PEG-type nonionic surfactants and imidazolium-based ILs which have shown that oxygen atoms in the PEG chains can establish H-bonds with the IL cations (in particular with the acidic proton at C2 of the imidazolium ring) in competition with IL anions.[91,92] The carbon atoms of the alkyl chain of the IL cation are present only at a second solvation layer around TEG (Figure 4, panels c and d). Some association of the less polar moiety of $[C_2mim]^+$ to the carbon atoms of the TEG chain is also detected at larger distances with a strength following the order C4(TEG) > C3(TEG) ≈ C2(TEG) ≈ C1(TEG) (Figure S6, Supporting Information).

The picture that emerges from the RDFs is that the most relevant interactions in the first solvation sphere of the polymer consist of the chloride anions and the less acidic protons of the imidazolium ring of the cation (H4) around the OH group, and the more acidic proton of the imidazolium ring (H2) around the O1 atom of TEG. The other ether oxygen atoms of the polymer do not significantly interact with the anion nor with the cation of the IL. In order to better visualize the molecular scenario described, the spatial distribution functions (SDFs) calculated for the system [C_2mim]Cl/TEG are provided in Figures 5 and 6. The SDF regions for the O1 atom of TEG are located quite near H2 atom of the cation (Figure 5). The SDF regions for the anion (Figure 6) are mainly located around the hydroxyl group of TEG, consistently with the data provided in Figure 3 and discussed above. These results are in agreement with literature reports where it has been shown that the imidazolium ring hydrogen atoms (particularly C2−H) can bind to the ether oxygens and to a lesser extent to the terminal −OH groups of PEG[27,93] and that the −OH groups can form strong H-bonds with the chloride ions.[93,94] It is worth noting that while the anion−cation interactions (particularly the H2···Cl^- hydrogen bonding) are stronger than the IL−TEG interactions described they allow, nevertheless, interactions between the IL ions and the polymer since a fraction of the IL will always be dissociated. It is also worth noting that the conformational flexibility of PEG chains[29] is a well-known characteristic of these polymers and can add complexity to the interactions that occur in these binary systems. In fact, the preferred conformations adopted by the TEG molecule are

dx.doi.org/10.1021/jp501718w | J. Phys. Chem. B 2014, 118, 4615−4629

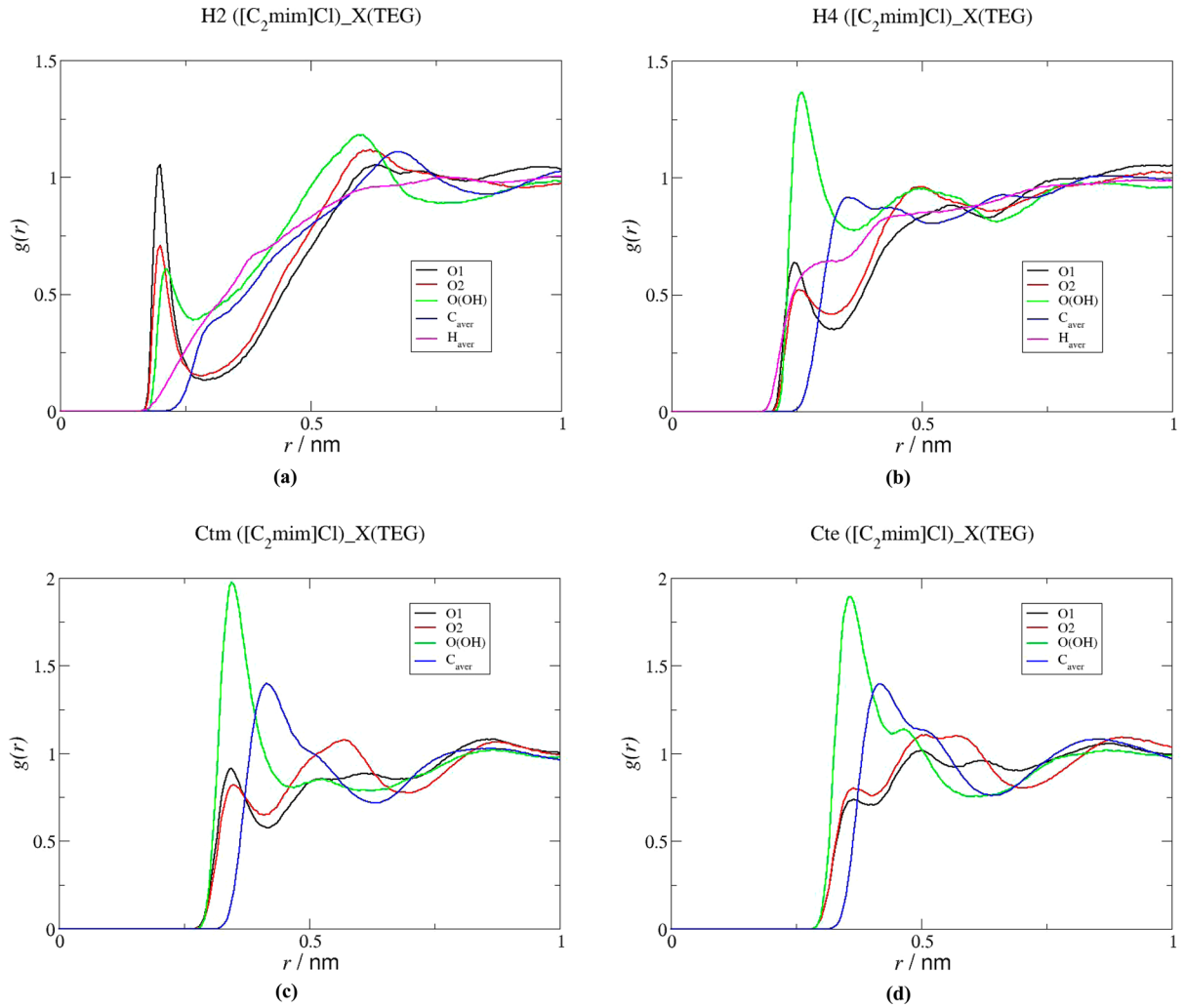

Figure 4. Radial distribution functions between selected atoms of the cation of [C_2mim]Cl and different regions of TEG. H_{aver} refers to the averaged interaction between the chloride anion and the H1, H2, H3, and H4 atoms of TEG, and C_{aver} refers to the averaged interaction between the chloride anion and the C1, C2, C3, and C4 atoms of TEG.

those in which the carbon chain is extended, and no intramolecular interactions are established. Some TEG molecules, however, present intramolecular hydrogen bonds involving the terminal OH groups and the ether oxygens of the polymer. Figure S7 of the Supporting Information provides a picture of this molecular scenario. In the absence of negative charges in the vicinity of the H atom, it is likely that (−OH)···(−O−) intramolecular bonds are established between the terminal OH group and the nearest ether oxygen atom or even (−OH)···(−OH) intra or intermolecular interactions. Nevertheless, in the presence of the IL (i.e., with the negative charges of the chloride ion present in the vicinity of the polymer) this molecular scenario is rather less probable since the hydrogen bonds established with the IL anion are extremely stable (Figures 3−6). There are even cases where two OH groups of two distinct TEG molecules bind to the same chloride ion (central region in Figure S7, Supporting Information). Moreover, the solvent accessible surface was pointed out as the major factor governing the molecular interactions occurring in the systems.[61] This will certainly determine the availability of some groups to interact with the IL relatively to the others.

To further explore the molecular mechanisms that govern the mutual solubility of ILs and PEGs, and to evaluate the effect of the length of the alkyl chain of the cation on the solubility behavior of these systems, further simulation results were obtained in this work for [C_1mim]Cl/TEG, [C_4mim]Cl/TEG, and [C_6mim]Cl/TEG (Figures S8−S13, Supporting Information). The interactions between the anion and the TEG protons (Figure S14, Supporting Information) and the interactions between H4 and O(OH) (Figure S15, Supporting Information) are not significantly affected by the length of the alkyl chain of the cation; however, the strength of the interactions established between H2 and O1 (Figure S16, Supporting Information) and Ct and O(OH) (Figure S17, Supporting Information) decrease with the increase of the length of the alkyl chain of the IL cation. This decrease is very likely steric in origin, as explained below.

Moreover, as shown in Figure 7 and Figures S9, S11, and S13 in the Supporting Information, there is some association of the alkyl chain of the cation to the apolar moieties of TEG. With the exception of [C_4mim]Cl, the strength of the interactions of the terminal carbon atoms of the cation with the internal carbon atoms of TEG decreases with the increase of the alkyl side chain length of the IL. As confirmed by the values reported in Table 1, for the ILs comprising longer chains, the electrostatic forces between the anion and the cation are

dx.doi.org/10.1021/jp501718w | J. Phys. Chem. B 2014, 118, 4615−4629

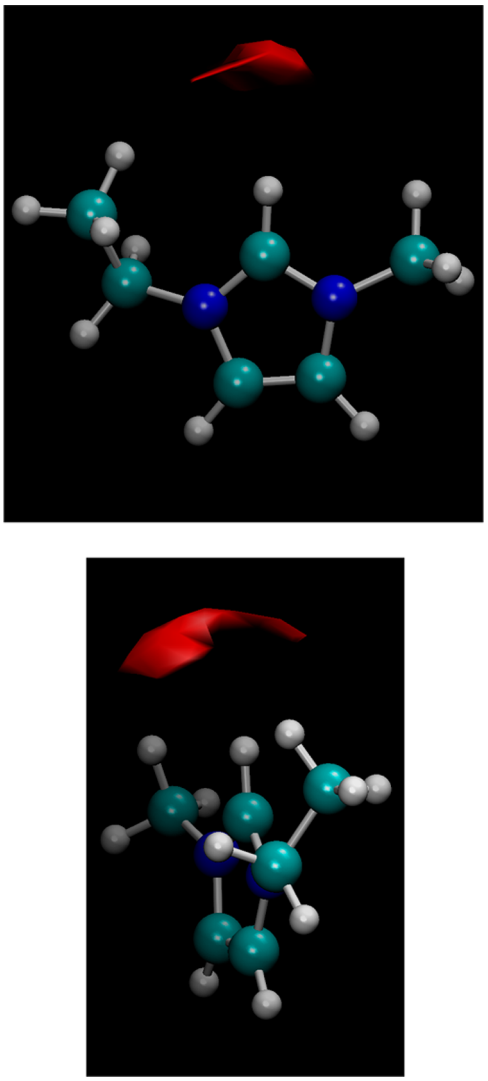

Figure 5. Frontal and side views of the spatial distribution function (SDF) for the O1 atom of TEG (red regions) around the cation of $[C_2mim]Cl$. Light blue, dark blue, and white spheres represent carbon, nitrogen, and hydrogen atoms, respectively.

weaker and correlate with experimental evidence.[95] As a result, the attraction of the cation to the anion located in the first solvation sphere is less pronounced. Consequently, the interactions of the cation with O1 (Figure S16, Supporting Information), with the hydroxyl (Figure S17, Supporting Information), and with the methylene (Figure 7) groups of TEG decrease with increasing cation alkyl chain length, due to steric effects. The association of the apolar moieties of the cation to the ether oxygen atoms of the TEG chain is not significant (Figure S18, Supporting Information) for all the systems. Quantitative support for the molecular scenario described can be obtained from the values of the Lennard-Jones and Coulomb terms of the interaction energies provided in Table 1, which show that the increase of the IL alkyl chain leads to a decrease in the IL cation−IL anion and TEG−IL anion interactions and to an increase of the interactions of TEG with the IL cation.

The type and strength of the molecular interactions inferred from the simulation results here reported are in good agreement and support the effect of the increase of the cation alkyl chain length on the phase behavior of binary mixtures of

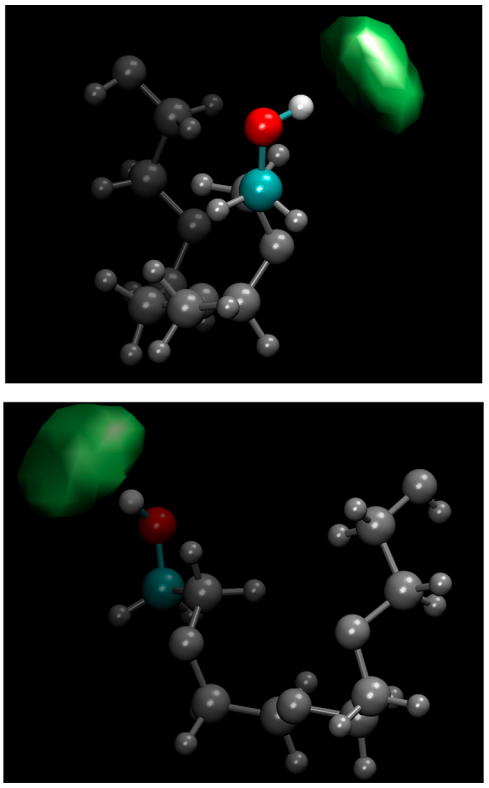

Figure 6. Selected views of the spatial distribution function (SDF) for the Cl^- anion (green regions) around the O(OH) group of TEG. White, red, and light blue spheres highlight the terminal hydrogen, oxygen, and carbon atoms, respectively, while the gray spheres are used to represent the rest of the atoms in the TEG chain.

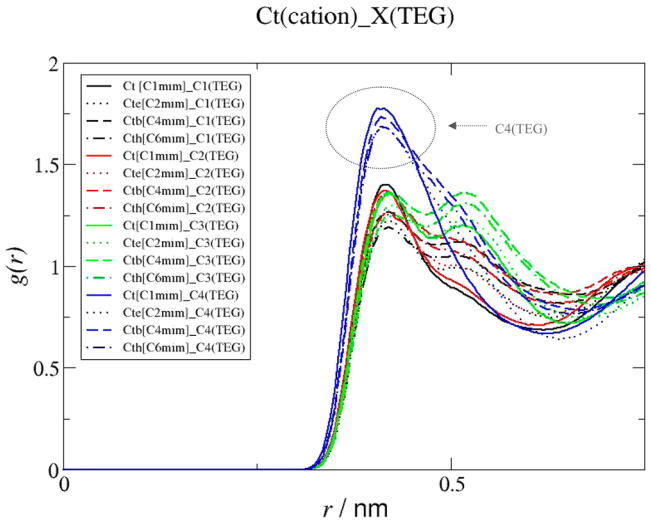

Figure 7. Comparison of the RDFs for the interactions of the carbon atoms of TEG and the terminal alkyl chain carbon atom of the cation of $[C_1mim]Cl$, $[C_2mim]Cl$, $[C_4mim]Cl$, and $[C_6mim]Cl$.

ILs and PEGs as described by Rodriguez et al.,[34] showing that for a fixed PEG molecular weight the increase on the cation alkyl chain length would enhance the mutual solubilities. The results reported here also support the influence of the increase of the molecular weight of PEG reported by Rodriguez et al.,[34] though this effect has not been studied in this work. Actually, with the hydrogen-bonding between Cl^- and the −OH group of TEG being the main interaction controlling the mutual

dx.doi.org/10.1021/jp501718w | J. Phys. Chem. B 2014, 118, 4615−4629

Table 1. Values (kJ·mol^{-1}) of the Lennard-Jones (LJ) and Coulomb (Coul) Terms of the Energies Calculated for the Interactions (IL Cation−IL anion), (TEG−IL anion), and (TEG−IL cation) for the Different Binary Systems under Study

		[C_1mim]Cl	[C_2mim]Cl	[C_4mim]Cl	[C_6mim]Cl
IL cation−IL anion	LJ	773.6	707.3	609.5	579.0
	Coul	−8376.7	−7912.1	−7711.0	−7583.9
TEG−IL anion	LJ	82.3	110.3	136.5	118.3
	Coul	−4688.3	−4690.0	−4517.8	−4244.71
TEG−IL cation	LJ	−3517.9	−4108.2	−5067.7	−5737.7
	Coul	−1816.0	−1573.8	−1309.8	−1137.3

solubilities of the ILs and the glycol (and thus, of PEG polymers), the decrease in the mutual solubility of IL and PEG with the increase of the molecular weight of the polymer can be explained in terms of the decrease in the number of OH groups per EO group with increasing PEG molecular weight.

4.2.2. Ternary Systems. To obtain further insight into the molecular mechanisms that control the formation of PEG-IL-based ABS and determine the influence of the length of the alkyl chain of the IL, we have examined the simulation results obtained for the ([C_1mim]Cl/[C_2mim]Cl/[C_4mim]Cl/[C_6mim]Cl + TEG + water) ternary systems.

We first investigated if the dehydration of TEG caused by the formation of hydration complexes of the ions is, as in typical salt-based ABS, controlling the phase behavior. With that purpose, we performed additional MD calculations of TEG/water and TEG/Na_2SO_4/water systems, under the same simulation conditions used for the TEG/ILs. Figure 8 shows

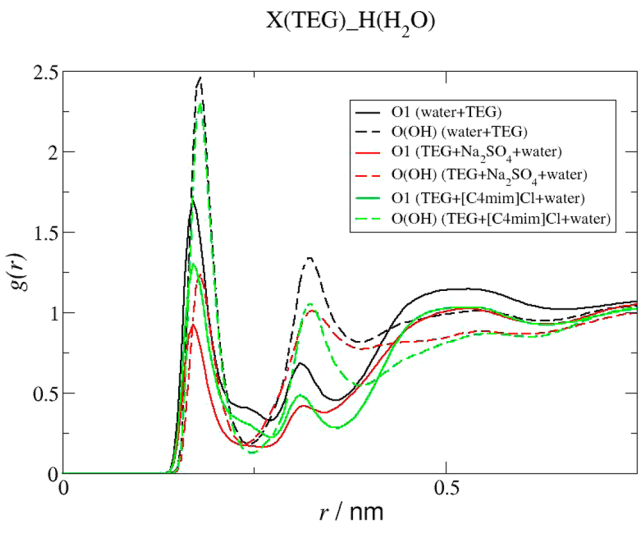

Figure 8. Comparison of the RDFs for the interaction of the hydrogen atoms of water with the O1 and O(OH) atoms of TEG for the systems (TEG + water), (TEG + Na_2SO_4 + water), and (TEG + [C_4mim]Cl + water).

the RDFs corresponding to the main interactions of the polymer with water, for the binary aqueous solution of TEG, and for the ternary mixtures containing either Na_2SO_4 or [C_4mim]Cl. The relative intensities of the RDF peaks indicate that the hydrogen bonds established between TEG and water, which are very strong for the binary system, are still significant in the TEG/IL/water ternary system, while they are much less evident for the TEG/Na_2SO_4/water mixture. While the solvation of TEG is slightly decreased by the presence of the IL, the dehydration effect is not as pronounced as in the case of the systems involving the inorganic salt. The cation chain length has no significant effect upon the dehydration of TEG caused by the IL as shown in Figure S19 (Supporting Information). This excludes the hypothesis that phase demixing of the PEG/IL-based ABS is ruled solely by the dehydration of the polymer. This is consistent with the suggestion by Freire et al.[32] that the interactions between PEG and ILs play an important role in the phase behavior of this type of ABS and with novel evidence provided by experimental and MD results which show that polymer/IL-based ABS are not a result of a salting-out effect of the IL over the polymer.[40]

The most relevant RDFs for the interactions occurring in aqueous mixtures of [C_4mim]Cl and TEG are displayed in Figures 9 and 10, and reveal a molecular scenario very distinct

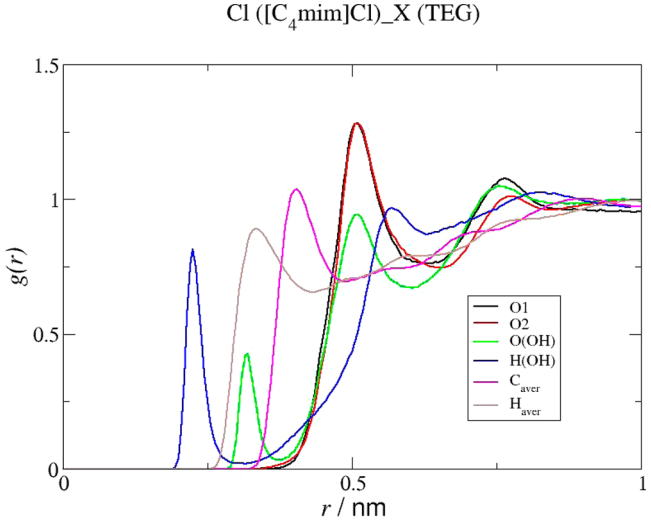

Figure 9. Radial distribution functions between the anion of [C_4mim]Cl and different regions of TEG for (TEG + [C_4mim]Cl + water) ternary mixtures. H_{aver} refers to the averaged interaction between the chloride anion and the H1, H2, H3, and H4 atoms of TEG, and C_{aver} refers to the averaged interaction between the chloride anion and the C1, C2, C3, and C4 atoms of TEG.

from that observed for the binary systems discussed in the previous section. The introduction of water into the mixtures displaces most of the hydrogen bonding between the chloride anion and the TEG hydroxyl group that was a strongly dominant feature on the binary system. The system is now characterized by a near absence of the anion from the first solvation layer of the polymer, as suggested by the RDF peaks referring to the contact pairs $Cl^-\cdots X$(TEG) presented in Figure 9. The cation, with the exception of a minor hydrogen bonding of the H2 of the cation to the O1 atom of TEG, suggested by a clear, though weak, RDF peak shown in Figure 10a, mainly interacts with the less polar moiety of the polymer through the

dx.doi.org/10.1021/jp501718w | J. Phys. Chem. B 2014, 118, 4615−4629

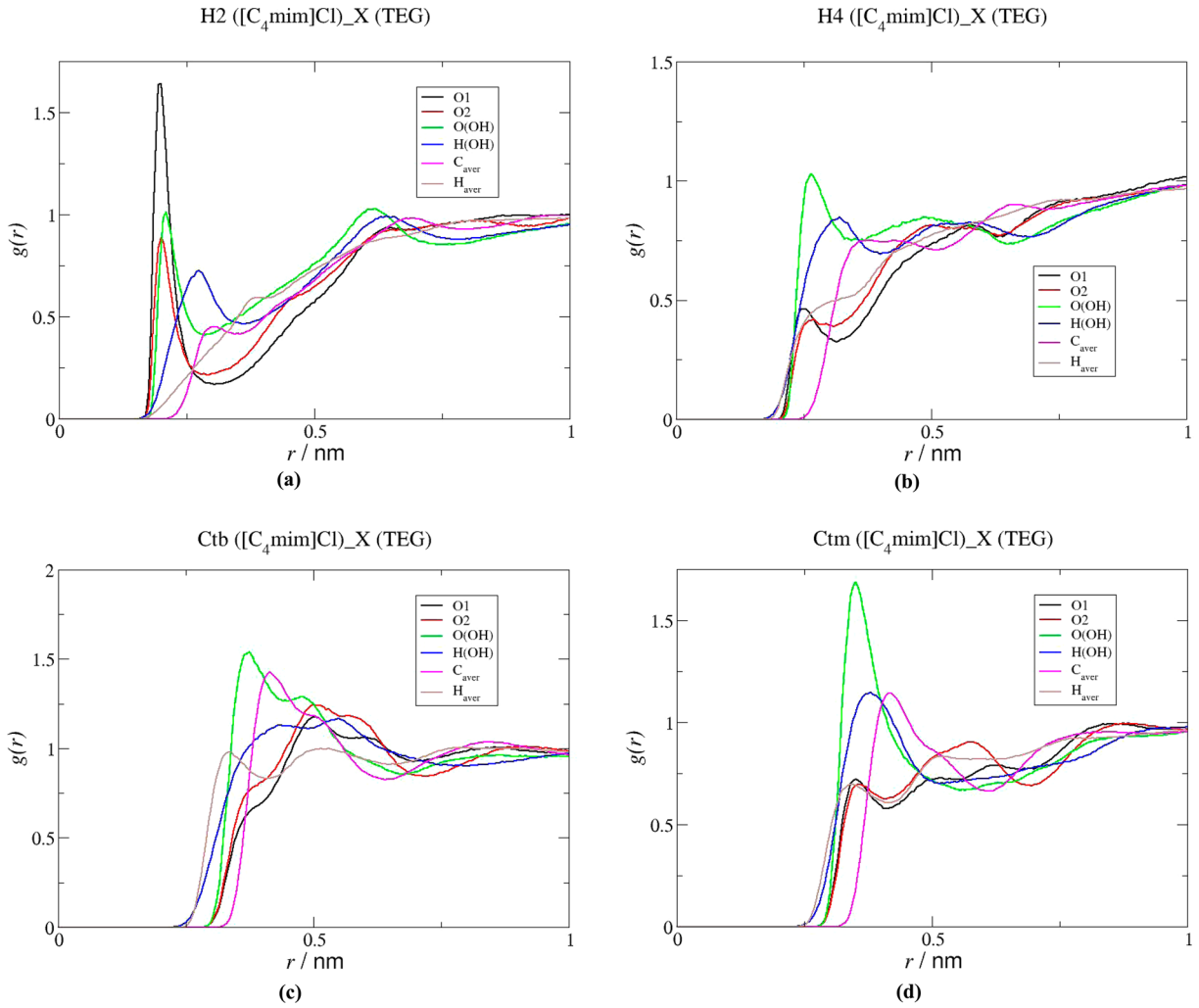

Figure 10. Radial distribution functions between selected atoms of the cation of [C_4mim]Cl and different regions of TEG for (TEG + [C_4mim]Cl + water) ternary mixtures. H_{aver} refers to the averaged interaction between the chloride anion and the H1, H2, H3, and H4 atoms of TEG, and C_{aver} refers to the averaged interaction between the chloride anion and the C1, C2, C3, and C4 atoms of TEG.

alkyl side chain (please refer also to Figures S20 and S21, Supporting Information).

The molecular picture described is consistent with the ^{1}H NMR chemical shift deviations analyzed above and with evidence reported before[40] for the influence of concentration on the interactions established between TEG and [C_4mim]Cl, which show a decrease in the $Cl^-\cdots$H(OH) (TEG) interactions, a slight decrease in the association of the hydrogen atoms of the imidazolium ring to the oxygen atoms of TEG, and no significant differences in the interactions between the apolar moieties of the cation and the polymer, with increasing water content. These data clearly support the idea that the introduction of water leads to the replacement of the hydrogen bonds formed between the IL ions and TEG by more favorable and stronger water−IL anion hydrogen bonds, in what we named a "washing-out" phenomenon.[40]

Similar interaction patterns are observed for the mixtures containing [C_6mim]Cl (Figures S22 and S23, Supporting Information). The systems comprising the ILs with short alkyl chains, [C_2mim]Cl (Figures S24 and S25, Supporting Information) and particularly [C_1mim]Cl (Figures S26 and S27, Supporting Information), however, present distinct behavior. The differences found among the systems studied, related to the influence of the length of the alkyl chain of the cation, will be discussed below.

To evaluate the influence of the alkyl chain length of the cation of the IL, the RDFs calculated in this work for [C_1mim]Cl/TEG/water, [C_2mim]Cl/TEG/water, [C_4mim]-Cl/TEG/water, and [C_6mim]Cl/TEG/water were compared, and the experimental data available for the phase behavior of ternary aqueous mixtures of ILs and PEGs[32,36,40] was considered. The analysis of the RDFs displayed in Figures 11 and 12 highlights the following main aspects: the anion of the IL avoids the vicinity of TEG in all of the ternary systems considered, as indicated by the depletion observed in the RDF peaks of Figure 11. As far as the cation is concerned, Figure 12a and b reveal that the association of the polar H2 atom of the imidazolium ring with the O1 ether oxygen of TEG is more significant for the system comprising [C_6mim]Cl, and almost no interactions are observed between H4(cation) and O(OH)-(TEG) in the case of the aqueous mixtures containing [C_4mim]Cl and [C_6mim]Cl. On the contrary, some (weak) binding of the hydrogen atoms of the imidazolium ring of [C_2mim]Cl and [C_1mim]Cl to the oxygen atoms of TEG are observed, particularly in the case of the latter IL.

The most remarkable differences found among the systems under study are related to the binding of TEG to the cation, at

dx.doi.org/10.1021/jp501718w | J. Phys. Chem. B 2014, 118, 4615−4629

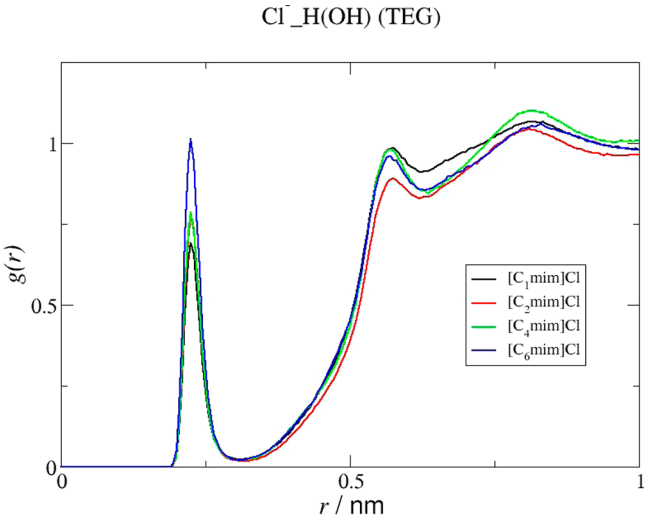

Figure 11. Radial distribution functions between the IL anion and the hydroxyl group of TEG for the different ternary mixtures studied in this work.

the level of the apolar moieties of both species. In fact, as suggested by the relative intensities of the RDF peaks of Figure 12c, d, e, and f and from the data presented in Figure 10, and Figures S22 to S27 in Supporting Information, those interactions are almost absent in the case of [C_1mim]Cl and [C_2mim]Cl but are clearly observed for [C_4mim]Cl and [C_6mim]Cl mixtures, being more intense for the methyl groups further away from the imidazolium ring. These interactions are of a hydrophobic nature and are similar or only slightly weaker than those observed for the binary systems suggesting that, unlike the interactions of the anion, these are not significantly modified by the presence of water. These interactions thus become dominant in the formation of ABS. Here, ABS formation no longer results from a salting-out of the polymer over the IL or the IL over the polymer, as in the salt containing systems, but from the polymer−IL mutual miscibilities that are controlled by the hydrophobic interactions established between the cation alkyl chain and the less polar moiety of the PEG.

The more favorable affinity of TEG and the ILs with longer alkyl side chains is confirmed by the values obtained for the energies of the (TEG-IL cation) interactions (Table 2), which are less positive for [C_4mim]Cl and [C_6mim]Cl. However, the results provided in Table 2 reveal that in the presence of the ILs with longer alkyl chains, the hydration of the anion is less favorable, while that of the cation is more pronounced. In addition, the cation−anion association decreases with the increase of the cation alkyl chain length due to steric effects.

Although for all of the systems studied the simulation data show that the phase behavior of PEG/IL-based ABS is controlled by the interactions established between the polymer and the IL, distinct features are observed for the mixtures containing the ILs with short alkyl side chains when compared to those comprising ILs with longer alkyl side chains. In fact, while in the case of the longer alkyl chain derivatives those dominant interactions have a hydrophobic character, for mixtures containing [C_1mim]Cl and [C_2mim]Cl, the polymer−IL association is mainly electrostatic, as suggested by the RDFs depicted in Figure 12, which show that the peaks corresponding to the H4(cation)···O(OH)(TEG) contact pair are stronger for [C_1mim]Cl and [C_2mim]Cl than for the other ILs (Figure 12b) and that the Ct([C_1mim]/[C_2mim]Cl)-Cx(TEG) interactions are almost nonexistent.

Furthermore, with the exception of a weak H4/O(OH) association, the interactions established in [C_2mim]Cl systems are actually not significant, while in the case of [C_1mim]Cl, a clear binding of H2 of the cation to the O1 atom of TEG is found (Figure 12a). These results explain the decrease in the ability of the ILs to produce ABS with the increase of their alkyl side chain with the [C_2mim]-, [C_4mim]-, and [C_6mim]-based ILs and the unexpected behavior of [C_1mim]Cl.[32] Indeed, because (due to its small size) $[C_1mim]^+$ is able to establish additional (and stronger) electrostatic interactions with the polymer, its affinity with TEG is enhanced. As a consequence, this IL has a lower capacity to promote ABS and does not follow the trend experimentally observed for [C_2mim]Cl, [C_4mim]Cl, and [C_6mim]Cl,[32] which may be interpreted in terms of an increase of the strength of the IL/polymer interactions, almost nonexistent in the case of [C_2mim]Cl.

In summary, the results obtained for the TEG ternary systems suggests that the phase demixing in PEG-IL type ABS is governed by the mutual solubilities between the polymer and the ILs. More specifically, the interactions occurring between the less polar moieties of both species control the phase behavior of the ternary systems comprising ILs with longer alkyl chains, while electrostatic interactions rule the formation of ABS composed of [C_1mim]Cl and [C_2mim]Cl. Contrarily to [C_1mim]Cl mixtures in which the IL, due to the small size of the cation, establishes stronger (electrostatic) interactions with the polymer, in the case of [C_2mim]Cl, [C_4mim]Cl, and [C_6mim]Cl systems, the introduction of water leads to almost complete replacement of the H-bonding between TEG and the IL by more favorable and stronger water−IL hydrogen bonds, as if "washed away" by water.[40] The H-bonds established with the anion and with the cation become less important, and the hydrophobic interactions between the cation alkyl chain and the less polar moiety of the PEG become dominant. As a result, two aqueous phases are formed: one an IL-rich phase (the IL becomes more hydrated as well) and the other a TEG-rich phase.

[C_2mim]Cl is only able to establish minor interactions with the hydroxyl group of TEG, while ILs with longer alkyl chains are more hydrophobic and are thus able to establish stronger interactions between the apolar groups of their cations and the less polar moieties of the polymer. As a consequence, the affinity of PEG and these ILs becomes more significant, and therefore, their ability to promote ABS is smaller, as experimentally observed.[32] An increase in the cation side chain also results in a decrease in the cation/anion attraction,[95] which might also contribute to an enhanced availability of the ions to interact with TEG (cation) and with water molecules (anion).

It is worth noting that the effect of the length of the cation alkyl chain on the hydration of the ion (the longer the chain, the more hydrated is the cation) constitutes further evidence for the conclusion that the molecular mechanisms underlying the formation of PEG-IL-based ABS are different from those controlling typical ABS, in which the phase behavior is dominated by the salting-out effect that results from the ability of the ions to form complexes with water. This is in agreement with interpretations provided earlier[32,40] but in stark contradiction with more conventional explanations[96−98] based on the salting-out/salting-in nature of the ILs as compared to salts,

dx.doi.org/10.1021/jp501718w | J. Phys. Chem. B 2014, 118, 4615−4629

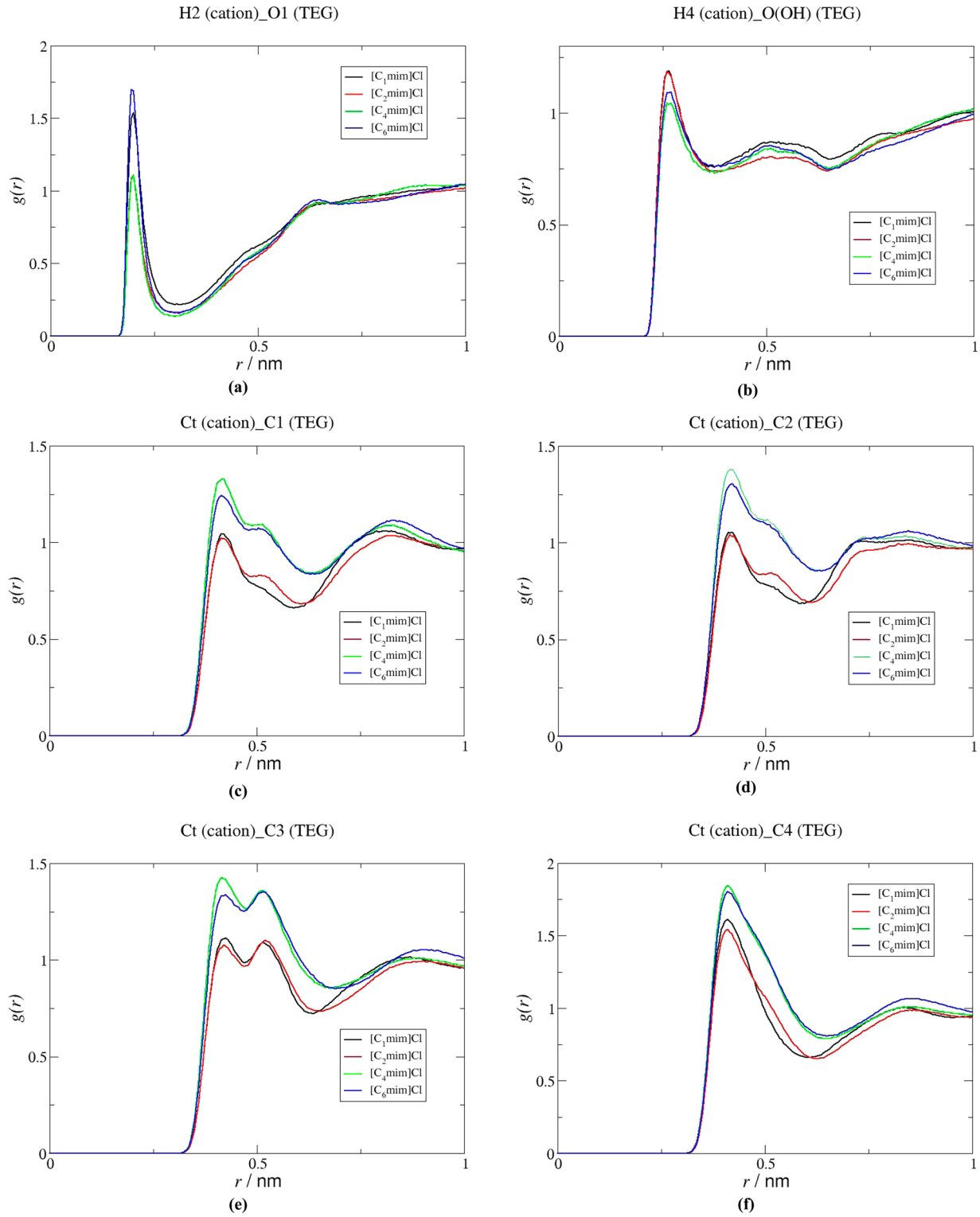

Figure 12. Radial distribution functions between selected atoms of the cation and different regions of TEG for the different ternary mixtures studied in this work.

where only water−PEG, water−water, and IL−water interactions are considered.

5. CONCLUSIONS

^{1}H NMR spectroscopy and molecular dynamics simulations studies were performed in order to investigate the interactions that control the mutual solubilities between ILs and PEGs and the formation of PEG/IL-based ABS. The MD simulation evidence gathered for the TEG + IL binary systems revealed that the hydrogen bonding between Cl^- and the −OH group of TEG is the main interaction controlling the mutual solubilities between the IL and the polymer. For ILs comprising longer alkyl side chains, the cation−anion interactions are less pronounced, and therefore, the attraction of the cation to the

dx.doi.org/10.1021/jp501718w | J. Phys. Chem. B 2014, 118, 4615−4629

Table 2. Values (kJ·mol^{-1}) of the Lennard-Jones (LJ) and Coulomb (Coul) Terms of the Energies Calculated for the Interactions (IL Anion−Water), (IL Cation−Water), (TEG−IL Cation), and (TEG−Water) for the Different Ternary Systems under Study

		[C_1mim]Cl	[C_2mim]Cl	[C_4mim]Cl	[C_6mim]Cl
IL anion−water	LJ	1854.8	1833.7	1798.3	1813.7
	Coul	−11239.1	−11259.5	−11010.4	−11137.4
IL cation−water	LJ	−671.6	−829.1	−978.2	−1071.8
	Coul	−461.9	−376.8	−329.0	−343.7
TEG−IL cation	LJ	−1696.9	−1872.6	−2500.5	−2941.1
	Coul	−984.2	−805.6	−709.4	−717.3
TEG−water	LJ	−725.9	−670.9	−589.2	−538.0
	Coul	−5610.4	−5260.5	−5438.2	−5107.1
IL cation−IL anion	LJ	70.4	43.7	15.0	−9.4
	Coul	−3442.2	−3402.4	−3347.4	−3201.3

anion located in the first solvation sphere is less significant. Consequently, the interactions of the cation with the different groups of TEG are weaker.

The MD data obtained for the TEG/IL/water ternary mixtures showed that, contrary to the salt containing systems, ABS formation does not result from a salting-out of the polymer by the IL or the IL by the polymer but from the polymer−IL mutual miscibilities. These are controlled by electrostatic interactions in the case of mixtures containing ILs with short alkyl chains and by the hydrophobic interactions established between the less polar moieties of both species in systems comprising ILs with longer alkyl chains. In this case, the simulation results showed that the introduction of water into the mixtures leads to the complete replacement of the hydrogen bond between the chloride anion and the TEG hydroxyl group by Cl^-/water H-bonding and that the formation of PEG/IL-based ABS becomes controlled by the hydrophobic interactions occurring between the cation alkyl chain and the less polar moieties of the polymer. These interactions are more intense for ILs with longer alkyl chains and are similar to those observed for the binary systems, suggesting that they are not significantly modified by the presence of water.

The simulation results here reported are in good agreement with the ^{1}H NMR chemical shift deviations observed for aqueous solutions of PEG-200 and [C_4mim]Cl, and constitute a further evidence for a "washing-out" mechanism behind the phase separation of PEG/IL mixtures when water is introduced into the system. The molecular interpretations derived from the data reported in this work constitute a relevant contribution for the understanding of the formation of ABS and for the development of (bio)technological applications using combinations of ILs and PEGs.

■ ASSOCIATED CONTENT

Supporting Information

Densities for binary mixtures of water and TEG calculated from the MD simulations; full set of electrostatic charges for the ILs and TEG model; compositions (wt %) of the mixtures at which the MD calculations and the ^{1}H NMR experiments were performed; compositions of the biphasic region of the [C_4mim]Cl/PEG/water phase diagram at which the additional MD simulations were performed; comparison of the experimental and calculated densities for binary mixtures of water and TEG; compositions of the experimental phase diagrams of the ABS composed of PEG 1500 and [C_4mim]Cl at which the ^{1}H NMR experiments and the MD simulations were performed; ^{1}H NMR chemical shift deviations between PEG-200 and [C_4mim]Cl; radial distribution functions between the anion and cation of [C_2mim]Cl and the hydrogen and carbon atoms of TEG; snapshot from a simulation of ([C_4mim]Cl + TEG); radial distribution functions between the anions and selected atoms of the cations of [C_1mim]Cl/[C_4mim]Cl/[C_6mim]Cl and different molecular regions of TEG for the binary systems; comparison of the radial distribution functions for the interactions of selected groups of TEG with the anions and with selected atoms of the cations for the binary systems and with water for the different ternary systems; radial distribution functions between the anion and cation of [C_4mim]Cl and the hydrogen and carbon atoms of TEG for (TEG + [C_4mim]Cl + water) ternary mixtures; radial distribution functions between the anions and selected atoms of the cations of [C_1mim]Cl/[C_2mim]C_l//[C_6mim]Cl and different molecular regions of TEG for the ternary systems, and the complete author list for ref 84. This material is available free of charge via the Internet at http://pubs.acs.org.

■ AUTHOR INFORMATION

Corresponding Author

*Tel: +351-234-370200. Fax: +351-234-370084. E-mail: jcoutinho@ua.pt.

Notes

The authors declare no competing financial interest.

■ ACKNOWLEDGMENTS

This work was financed by national funding from FCT (Fundação para a Ciência e a Tecnologia) through the project PTDC/QUI-QUI/121520/2010, by FEDER fundings through program COMPETE and by national fundings through FCT in the ambit of project CICECO - FCOMP-01-0124-FEDER-037271 (Ref. FCT Pest-C/CTM/LA0011/2013). We also acknowledge FCT for the postdoctoral grant SFRH/BPD/44926/2008 to L.I.N.T. M.G.F. and J.R.B.G. acknowledge FCT for the 2012 FCT Investigator Program positions.

■ REFERENCES

(1) Powell, G. M. *Handbook of Water Soluble Gums and Resins*; McGraw-Hill: New York, 1980.

(2) Herold, D.; Keil, K.; Burns, D. E. Oxidation of Polyethylene Glycols by Alcohol Dehydrogenase. *Biochem. Pharmacol.* **1989**, *38*, 73−76.

(3) Bridges, N. J.; Gutowski, K. E.; Rogers, R. D. Investigation of Aqueous Biphasic Systems formed from Solutions of Chaotropic Salts

with Kosmotropic Salts (Salt-Salt ABS). *Green Chem.* **2007**, *9*, 177−183.
(4) Harris, J. M.; Chess, R. B. Effect of Pegylation on Pharmaceuticals. *Nat. Rev. Drug Discovery* **2003**, *2*, 214−221.
(5) Jeon, S. I.; Lee, J. H.; Andrade, J. D.; de Gennes, P. G. Protein-Surface Interactions in the Presence of Polyethylene Oxide: I. Simplified Theory. *J. Colloid Interface Sci.* **1991**, *142*, 149−158.
(6) Drohmann, C.; Beckman, E. J. Phase Behavior of Polymers Containing Ether Groups in Carbon Dioxide. *J. Supercrit. Fluids* **2002**, *22*, 103−110.
(7) Ding, J.; Maitra, P.; Wunder, S. L. Characterization of the Interaction of Poly(ethylene oxide) with Nanosize Fumed Silica: Surface Effects on Crystallization. *J. Polym. Sci., Part B: Polym. Phys.* **2003**, *41*, 1978−1993.
(8) Batrakova, E. V.; Kabanov, A. V. Pluronic Bolock Copolymers: Evolution of Drug Delivery Concept from Inert Nanocarriers to Biological Response Modifiers. *J. Controlled Release* **2008**, *130*, 98−106.
(9) Viossat, B.; Greenaway, F. T.; Morgant, G.; Daran, J. C.; Dung, N. H.; Sorenson, J. R. J. Low-Temperature (180 K) Crystal Structures of Tetrakis-u-(niflumato)-di(aqua)dicopper(II) N,N-Dimethylformamide and N,N-Dimethylacetamide Solvates, Their EPR Properties, and Anticonvulsant Activities of These and Other Ternary Binuclear Copper(II)niflumate Complexes. *J. Inorg. Biochem.* **2005**, *99*, 355−367.
(10) Braun, A.; Stenger, P. C.; Warriner, H. E.; Zasadzinski, J. A.; Lu, K. W.; Taeusch, H. W. A Freeze-Fracture Transmission Electron Microscopy and Small Angle X-Ray Diffraction Study of the Effects of Albumin, Serum, and Polymers on Clinical Lung Surfactant Microstructure. *Biophys. J.* **2007**, *93*, 123−139.
(11) Robertson, J. W. F.; Rodrigues, C. G.; Stanford, V. M.; Rubinson, K. A.; Krasilnikov, O. V.; Kasianowicz, J. J. Single-Molecule Mass Spectrometry in Solution Using a Solitary Nanopore. *Proc. Natl. Acad. Sci. U.S.A.* **2007**, *104*, 8207−8211.
(12) Chen, J.; Spear, S. K.; Huddleston, J. G.; Rogers, R. D. Polyethylene Glycol and Solutions of Polyethylene Glycol as Green Reaction Media. *Green Chem.* **2005**, *7*, 64−82.
(13) Borodin, O.; Douglas, R.; Smith, G. D.; Trouw, F.; Petrucci, S. MD Simulations and Experimental Study of Structure, Dynamics, and Thermodynamics of Poly(ethylene oxide) and Its Oligomers. *J. Phys. Chem. B* **2003**, *107*, 6813−6823.
(14) Sasanauma, Y.; Ohta, H.; Touma, I.; Matoba, H.; Hayashi, Y.; Kaito, A. Conformational Characteristics of Poly(ethylene sulfide) and Poly(ethylene oxide): Solvent Dependence of Attractive and Repulsive Gauche Effects. *Macromolecules* **2002**, *35*, 3748−3761.
(15) Wick, C. D.; Theodorou, D. N. Connectivity-Altering Monte Carlo Simulations of the End Group Effects on Volumetric Properties of Poly(ethylene oxide). *Macromolecules* **2004**, *37*, 7026−7033.
(16) Comelli, F.; Ottani, S.; Vitalini, D.; Francesconi, R. A Calorimetric Study of Binary Mixtures Containing some Glycols and Polyglycols+Anisole at 308.15 K and at Atmospheric Pressure. *Thermochim. Acta* **2003**, *407*, 85−92.
(17) Kinart, C. M.; Klimczak, M.; Kinart, W. J. Volumetric and Dielectric Characterization and Analysis of Internal Structure of Binary Mixtures of 2-Ethoxyethanol with Ethylene Glycol, Diethylene Glycol, Triethylene Glycol, and Tetraethylene Glycol at T=(293.15, 298.15, and 303.15) K. *J. Mol. Liq.* **2009**, *145*, 8−13.
(18) Derkaoui, N.; Said, S.; Grohens, Y.; Olier, R.; Privat, M. PEG400 Novel Phase Description in Water. *J. Colloid Interface Sci.* **2007**, *305*, 330−338.
(19) Anderson, P. M.; Wilson, M. R. Developing a Force Field for Simulation of Poly(ethylene oxide) Based upon ab Initio Calculations of 1,2-dimethoxyethane. *Mol. Phys.* **2005**, *103*, 89−97.
(20) Vorobyov, I.; Anisimov, V. M.; Greene, S.; Venable, R. M.; Moser, A.; Pastor, R. W.; MacKerell, A. D. Additive and Classical Drude Polarizable Force Fields for Linear and Cyclic Ethers. *J. Chem. Theory Comput.* **2007**, *3*, 1120−1133.
(21) Dormidontova, E. E. Influence of End Groups on Phase Behavior and Properties of PEO in Aqueous Solutions. *Macromolecules* **2004**, *37*, 7747−7761.
(22) Clop, E. M.; Perillo, M. A.; Chattah, A. K. 1-H and 2-H NMR Spin Lattice Relaxation Probing Water: PEG Molecular Dynamics in Solution. *J. Phys. Chem. B* **2012**, *116*, 11953−11958.
(23) Wasserscheid, P.; Keim, W. Ionic Liquids-New "Solutions" for Transition Metal Catalysis. *Angew. Chem., Int. Ed.* **2000**, *39*, 3772−3789.
(24) Zakrzewska, M. E.; Bogel-Lukasik, E.; Bogel-Lukasik, R. Solubility of Carbohydrates in Ionic Liquids. *Energy Fuels* **2010**, *24*, 737−745.
(25) Domanska, U.; Bogel-Lukasik, R. Physicochemical Properties and Solubility of Alkyl-2-(hydroxyethyl)-dimethylammonium Bromide. *J. Phys. Chem. B* **2005**, *109*, 12124−12132.
(26) Paulechka, Y. U.; Kabo, G. J.; Blokhin, A. V.; Vydrov, O. A.; Magee, J. W.; Frenkel, M. Thermodynamic Properties of 1-Butyl-3-methyl imidazolium Hexafluorophosphate in the Ideal Gas State. *J. Chem. Eng. Data* **2003**, *48*, 457−462.
(27) Seddon, K. R. Ionic Liquids for Clean Technology. *J. Chem. Technol. Biotechnol.* **1997**, *68*, 351−356.
(28) Shin, J.-H.; Henderson, W. A.; Passerini, S. Ionic Liquids to the Rescue? Overcoming the Ionic Conductivity Limitations of Polymer Electrolytes. *Electrochem. Commun.* **2003**, *5*, 1016−1020.
(29) Triolo, A.; Russina, O.; Keiderling, U.; Kohlbrecher, J. Morphology of Poly(ethylene oxide) Dissolved in a Room Temperature Ionic Liquid: A Small Angle Neutron Scattering Study. *J. Phys. Chem. B* **2006**, *110*, 1513−1515.
(30) Sarkar, A.; Trivedi, S.; Pandey, S. Unusual Solvatochromism within 1-Butyl-3-methyl imidazolium Hexafluorophosphate + Poly(ethylene glycol) Mixtures. *J. Phys. Chem. B* **2008**, *112*, 9042−9049.
(31) Pereira, J. F. B.; Lima, A. S.; Freire, M. G.; Coutinho, J. A. P. Ionic Liquids as Adjuvants for the Tailored Extraction of Biomolecules in Aqueous Biphasic Systems. *Green Chem.* **2010**, *12*, 1661−1669.
(32) Freire, M. G.; Pereira, J. F. B.; Francisco, M.; Rodríguez, H.; Rebelo, L. P. N.; Rogers, R. D.; Coutinho, J. A. P. Insight into the Interactions that Control the Phase Behaviour of New Aqueous Biphasic Systems Composed of Polyethylene Glycol Polymers and Ionic Liquids. *Chem.—Eur. J.* **2012**, *18*, 1831−1839.
(33) Li, X.; Hou, M.; Zhang, Z.; Han, B.; Yang, G.; Wang, X.; Zou, L. Absorption of CO_2 by Ionic Liquid/Polyethylene Glycol Mixture and Thermodynamic Parameters. *Green Chem.* **2008**, *10*, 879−884.
(34) Rodríguez, H.; Francisco, M.; Rahman, M.; Sun, N.; Rogers, R. D. Biphasic Liquid Mixtures of Ionic Liquids and Polyethylene Glycols. *Phys. Chem. Chem. Phys.* **2009**, *11*, 10916−10922.
(35) Rodríguez, H.; Rogers, R. D. Liquid Mixtures of Ionic Liquids and Polymers as Solvent Systems. *Fluid Phase Equilib.* **2010**, *294*, 7−14.
(36) Visak, Z. P.; Lopes, J. N. C.; Rebelo, L. P. N. Ionic Liquids in Polyethylene Glycol Aqueous Solutions: Salting-in and Salting-out Effects. *Monatsh. Chem.* **2007**, *138*, 1153−1157.
(37) Pereira, J. F. B.; Vicente, F.; Santos-Ebinuma, V. C.; Araújo, J. M.; Pessoa, A.; Freire, M. G.; Coutinho, J. A. P. Extraction of Tetracycline from Fermentation Broth using Aqueous Two-Phase Systems composed of Polyethylene Glycol and Cholinium Based Salts. *Process Biochem.* **2013**, *48*, 716−722.
(38) Pereira, J. F. B.; Kurnia, K. A.; Cojocaru, O. A.; Gurau, G.; Rebelo, L. P. N.; Rogers, R. D.; Coutinho, J. A. P.; Freire, M. G. Molecular Interactions in Aqueous Biphasic Systems Composed of Polyethylene Glycol and Crystalline vs Liquid Cholinium-Based Salts. *Phys. Chem. Chem. Phys.* **2014**, *16*, 5723−5731.
(39) Pereira, J. F. B.; Rebelo, L. P. N.; Rogers, R. D.; Coutinho, J. A. P.; Freire, M. G. Combining Ionic Liquids and Polyethylene Glycols to Boost the Hydrophobic-Hydrophilic Range of Aqueous Biphasic Systems. *Phys. Chem. Chem. Phys.* **2013**, *15*, 19580−19583.
(40) Tomé, L. I. N.; Pereira, J. F. B.; Rogers, R. D.; Freire, M. G.; Gomes, J. R. B.; Coutinho, J. A. P. "Washing-Out" Ionic Liquids from Polyethylene Glycol to form Aqueous Biphasic Systems. *Phys. Chem. Chem. Phys.* **2014**, *16*, 2271−2274.
(41) Glass, J. E. *Hydrophilic Polymers. Performance with Environmental Acceptability*; American Chemical Society: Washington, DC, 1996.

(42) Romero, A.; Santos, A.; Tojo, J.; Rodríguez, A. Toxicity and Biodegradability of Imidazolium Ionic Liquids. *J. Hazard. Mater.* **2008**, *151*, 268−273.
(43) Couling, D. J.; Bernot, R. J.; Docherty, K. M.; Dixon, J. K.; Maginn, E. J. Assessing the Factors Responsible for Ionic Liquid Toxicity to Aquatic Organisms via Quantitative Structure-Property Relationship Modeling. *Green Chem.* **2006**, *8*, 82−90.
(44) Lund, M.; Vrbka, L.; Jungwirth, P. Specific Ion Binding to Non Polar Surface Patches of Proteins. *J. Am. Chem. Soc.* **2008**, *130*, 11582−11583.
(45) Heyda, J.; Vincent, J. C.; Tobias, D. J.; Dzubiella, J.; Jungwirth, P. Ion Specificity at the Peptide Bond: Molecular Dynamics Simulations of N-Methylacetamide in Aqueous Salt Solutions. *J. Phys. Chem. B* **2010**, *114*, 1213−1220.
(46) Klahn, M.; Lim, G. S.; Seduraman, A.; Wu, P. On the Different Roles of Anions and Cations in the Solvation of Enzymes in Ionic Liquids. *Phys. Chem. Chem. Phys.* **2011**, *13*, 1649−1662.
(47) Sagarik, K.; Dokmaisrijan, S. A Theoretical Study on Hydration of Alanine Zwitterions. *J. Mol. Struct. (THEOCHEM)* **2005**, *718*, 31−47.
(48) Hess, B.; van der Vegt, N. F. A. Cation Specific Binding with Surface Charges. *Proc. Natl. Acad. Sci. U.S.A.* **2009**, *106*, 13296−13300.
(49) Tritopoulou, E. A.; Economou, I. G. Molecular Simulation of Structure and Thermodynamic Properties of Pure Tri- and Tetra-Ethylene Glycols and their Aqueous Mixtures. *Fluid Phase Equilib.* **2006**, *248*, 134−146.
(50) Tomé, L. I. N.; Jorge, M.; Gomes, J. R. B.; Coutinho, J. A. P. Toward an Understanding of the Aqueous Solubility of Amino Acids in the Presence of Salts: A Molecular Dynamics Simulation Study. *J. Phys. Chem. B* **2010**, *114*, 16450−16459.
(51) Tomé, L. I. N.; Pinho, S. P.; Jorge, M.; Gomes, J. R. B.; Coutinho, J. A. P. Salting-in with a Salting-out Agent: Explaining the Cation Specific Effects on the Aqueous Solubility of Amino Acids. *J. Phys. Chem. B* **2013**, *117*, 6116−6128.
(52) Freire, M. G.; Neves, C. M. S. S.; Silva, A. M. S.; Santos, L. M. N. B. F.; Marrucho, I. M.; Rebelo, L. P. N.; Shah, J. K.; Maginn, E. J.; Coutinho, J. A. P. 1H-NMR and Molecular Dynamics Evidence for an Unexpected Interaction on the Origin of Salting-in/Salting-out Phenomena. *J. Phys. Chem. B* **2010**, *114*, 2004−2014.
(53) Tomé, L. I. N.; Jorge, M.; Gomes, J. R. B.; Coutinho, J. A. P. Molecular Dynamics Simulation Studies of the Interactions between Ionic Liquids and Amino Acids in Aqueous Solutions. *J. Phys. Chem. B* **2012**, *116*, 1831−1842.
(54) Batista, M. L. S.; Tomé, L. I. N.; Neves, C. M. S. S.; Rocha, E. M.; Gomes, J. R. B.; Coutinho, J. A. P. The Origin of the LCST on the Liquid-Liquid Equilibrium of Thiophene with Ionic Liquids. *J. Phys. Chem. B* **2012**, *116*, 5985−5992.
(55) Micaêlo, N. M.; Soares, C. M. Protein Structure and Dynamics in Ionic Liquids. Insights from Molecular Dynamics Simulation Studies. *J. Phys. Chem. B* **2008**, *112*, 2566−2572.
(56) Moreno, M.; Castiglione, F.; Mele, A.; Pasqui, C.; Raos, G. Interaction of Water with the Model Ionic Liquid [bmim][BF4]: Molecular Dynamics Simulations and Comparison with NMR Data. *J. Phys. Chem. B* **2008**, *112*, 7826−7836.
(57) Harper, J. B.; Lynden-Bell, K. M. Macrsocopic and Microscopic Properties of Solutions of Aromatic Compounds in an Ionic Liquid. *Mol. Phys.* **2004**, *102*, 85−94.
(58) Lee, H.; Venable, R. M.; MacKerell, A. D., Jr.; Pastor, R. W. Molecular Dynamics Studies of Polyethylene Oxide and Polyethylene Glycol: Hydrodynamic Radius and Shape Anisotropy. *Biophys. J.* **2008**, *95*, 1590−1599.
(59) Smith, G. D.; Yoon, D. Y.; Jaffe, R. L.; Colby, R. H.; Krishnamoorti, R.; Fetters, L. J. Conformations and Structures of Poly(oxyethylene) Melts from Molecular Dynamics Simulations and Small-Angle Neutron Scattering Experiments. *Macromolecules* **1996**, *29*, 3462−3469.
(60) de Oliveira, O. V.; Freitas, L. C. G. Molecular Dynamics Simulation of Liquid Ethlynene Glycol and Its Aqueous Solutions. *J. Mol. Strct. (THEOCHEM)* **2005**, *728*, 179−187.
(61) Oelmeier, S. A.; Dismer, F.; Hubbuch, J. Molecular Dynamics Simulations on Aqueous Two-Phase Systems-Single PEG-molecules in Solution. *BMC Biophysics* **2012**, *5*, 14−27.
(62) Hess, B.; Kutzner, C.; van der Spoel, D.; Lindahl, E. GROMACS 4: Algorithms for Highly Efficient, Load-Balanced, and Scalable Molecular Simulation. *J. Chem. Theor. Comput.* **2008**, *4*, 435−447.
(63) Hockney, R. W.; Goel, S. P. J.; Eastwood, J. W. Quiet High-Resolution Computer Models of a Plasma. *J. Comput. Phys.* **1974**, *14*, 148−158.
(64) Nosé, S. A Molecular Dynamics Method for Simulations in the Canonical Ensemble. *Mol. Phys.* **1984**, *52*, 255−268.
(65) Hoover, W. G. Canonical Dynamics: Equilibrium Phase-Space Distributions. *Phys. Rev. A* **1985**, *31*, 1695−1698.
(66) Parrinello, M.; Rahman, A. Polymorphic Transitions in Single Crystals: a New Molecular Dynamics Method. *J. Appl. Phys.* **1981**, *52*, 7182−7192.
(67) Essman, U.; Perela, L.; Berkowitz, M. L.; Darden, T.; Lee, H.; Pederson, L. G. A Smooth Parcticle Mesh Ewald Method. *J. Chem. Phys.* **1995**, *103*, 8577−8593.
(68) Hess, B.; Bekker, H.; Berendsen, H. J. C.; Fraaije, J. G. E. M. LINCS: A Linear Constraint Solver for Molecular Simulations. *J. Comput. Chem.* **1997**, *18*, 1463−1472.
(69) Maginn, E. J. Molecular Simulation of Ionic Liquids: Current Status and Future Oportunities. *J. Phys.: Condens. Matter* **2009**, *21*, 373101−373117.
(70) Hunt, P. A. The Simulation of Imidazolium-Based Ionic Liquids. *Mol. Simul.* **2006**, *32*, 1−10.
(71) Bhargava, B. L.; Balasubramanian, S.; Klein, M. L. Modelling Room Temperature Ionic Liquids. *Chem. Commun.* **2008**, 3339−3351.
(72) Batista, M. L. S.; Coutinho, J. A. P.; Gomes, J. R. B. Prediction of Ionic Liquids Properties through Molecular Dynamics Simulation. *Curr. Phys. Chem.* **2013**, DOI: 10.2174/18779468036661312132316O2.
(73) Jorgensen, W. L.; Tirado-Rives, J. Potential Energy Functions for Atomic-Level Simulations of Water and Organic and Biomolecular Systems. *J. Proc. Natl. Acad. Sci. U.S.A.* **2005**, *102*, 6665−6670.
(74) Berendsen, H. J. C.; Grigera, J. R.; Straatsma, T. P. The Missing Term in Effective Pair Potentials. *J. Phys. Chem.* **1987**, *91*, 6269−6271.
(75) Cadena, C.; Maginn, E. J. Molecular Simulation Study of Some Thermophysical and Transport Properties of Triazolium-Based Ionic Liquids. *J. Phys. Chem. B* **2006**, *110*, 18026−18039.
(76) Chandrasekhar, J.; Spellmeyer, D. C.; Joegensen, W. L. Energy Component Analysis for Dilute Aqueous Solutions of Lithium(1+), Sodium(1+), Fluoride(1-), and Chloride(1-) Ions. *J. Am. Chem. Soc.* **1984**, *106*, 903−910.
(77) Juneja, A.; Numata, J.; Nilsson, L.; Knapp, E. W. Merging Implicit with Explicit Solvent Simulations: Polyethylene Glycol. *J. Chem. Theory Comput.* **2010**, *6*, 1871−1883.
(78) Starovoytov, O. N.; Borodin, O.; Bedrov, D.; Smith, G. D. Development of a Polarizable Force Field for Molecular Dynamics Simulations of Poly(Ethylene Oxide) in Aqueous Solutions. *J. Chem. Theor. Comput.* **2011**, *7*, 1902−1915.
(79) http://compbio.biosci.uq.edu.au/atb (last accessed Feb 7, 2014).
(80) Tsuji, T.; Hiaki, T.; Hongo, M. Vapor-Liquid Equilibria of the Three Binary Systems: Water+Tetraethylene Glycol (TEG), Ethanol +TEG, and 2-Propanol+TEG. *Ind. Eng. Chem. Res.* **1998**, *37*, 1685−1691.
(81) Muller, E. M.; Rasmussen, P. Densities and Excess Volumes in Aqueous Poly(Ethylene Glycol) Solutions. *J. Chem. Eng. Data* **1991**, *36*, 214−217.
(82) Yu, Y.-X.; Liu, J.-G.; Gao, G.-H. Isobaric Vapor-Liquid Equilibria and Excess Volumes for the Binary Mixtures Water+Sulfolane, Water +Tetraethylene Glycol, and Benzene+Tetraethylene Glycol. *J. Chem. Eng. Data* **2000**, *45*, 570−574.
(83) Logotheti, G.-E.; Ramos, J.; Economou, I. G. Molecular Modeling of Imidazolium-Based [Tf2N-] Ionic Liquids: Microscopic Structure, Thermodynamic and Dynamic Properties, and Segmental Dynamics. *J. Phys. Chem. B* **2009**, *113*, 7211−7224.

(84) Frisch, M.; Trucks, G. W.; Schlegel, H. B.; Scuseria, G. E.; Robb, M. A.; Cheeseman, J. R.; Scalmani, G.; Barone, V.; Mennucci, B.; Petersson, G. A. et al. *Gaussian 09*, revision A.02; Gaussian, Inc.: Wallingford, CT, 2009.
(85) Morrow, T. I.; Maginn, E. J. Molecular Dynamics Study of the Ionic Liquid 1-n-Butyl-3-methylimidazolium Hexafluorophosphate. *J. Phys. Chem. B* **2002**, *106*, 12807−12813.
(86) Aqvist, J. Ion-Water Interaction Potentials Derived from Free Energy Perturbation Simulations. *J. Phys. Chem.* **1990**, *94*, 8021−8024.
(87) Cannon, W. R.; Pettitt, B. M.; McCammon, J. A. Sulfate Anion in Water: Model Structural, Thermodynamic, and Dynamic Properties. *J. Phys. Chem.* **1994**, *98*, 6225−6230.
(88) Ventura, S. P. M.; Neves, C. M. S. S.; Freire, M. G.; Marrucho, I. M.; Oliveira, J.; Coutinho, J. A. P. Evaluation of Anion Influence on the Formation and Extraction Capacity of Ionic Liquid-Based Aqueous Biphasic Systems. *J. Phys. Chem. B* **2009**, *113*, 9304−9310.
(89) Neves, C. M. S. S.; Ventura, S. P. M.; Freire, M. G.; Marrucho, I. M.; Coutinho, J. A. P. Evaluation of Cation Influence on the Formation and Extraction Capability of Ionic Liquid-Based Aqueous Biphasic Systems. *J. Phys. Chem. B* **2009**, *113*, 5194−5199.
(90) Freire, M. G.; Cláudio, A. F. M.; Araújo, J. M. M.; Coutinho, J. A. P.; Marrucho, I. M.; Canongia Lopes, J. N.; Rebelo, L. P. N. Aqueous Biphasic Systems: a Boost Brought About by Using Ionic Liquids. *Chem. Soc. Rev.* **2012**, *41*, 4966−4995.
(91) Inoue, T.; Misono, T. Cloud Point Phenomena for POE-Type Nonionic Surfactants in a Model Room Temperature Ionic Liquid. *J. Colloid Interface Sci.* **2008**, *326*, 483−489.
(92) Inoue, T.; Misono, T. Cloud Point Phenomena for POE-Type Nonionic Surfactants in Imidazolium-Based Ionic Liquids: Effect of Anion Species of Ionic Liquids on the Cloud Point. *J. Colloid Interface Sci.* **2009**, *337*, 247−253.
(93) Wang, L.; Chen, X.; Chai, Y.; Hao, J.; Sui, Z.; Zhuang, W.; Sun, Z. Lyotropic Liquid Crystalline Phases Formed in an Ionic Liquid. *Chem. Commun.* **2004**, 2840−2841.
(94) Remsing, R. C.; Swatloski, R. P.; Rogers, R. D.; Moyna, G. Mechanism of Cellulose Dissolution in the Ionic Liquid 1-n-Butyl-3-methylimidazolium Chloride: a 13C and 35/37Cl NMR Relaxation Study on Model Systems. *Chem. Commun.* **2006**, 1271−1273.
(95) Fernandes, A. M.; Rocha, M. A. A.; Freire, M. G.; Marrucho, I. M.; Coutinho, J. A. P.; Santos, L. M. N. B. F. Evaluation of Cation-Anion Interaction Strength in Ionic Liquids. *J. Phys. Chem. B* **2011**, *115*, 4033−4041.
(96) Wu, C.; Wang, J.; Pei, Y.; Wang, H.; Li, Z. Salting-Out Effect of Ionic Liquids on Poly(propylene glycol) (PPG): Formation of PPG +Ionic Liquid Aqueous Two-Phase Systems. *J. Chem. Eng. Data* **2010**, *55*, 5004−5008.
(97) Zafarani-Moattar, M. T.; Hamzehzadeh, S.; Nasiri, S. A New Aqueous Biphasic System Containing Polypropylene Glycol and a Water-Miscible Ionic Liquid. *Biotechnol. Prog.* **2012**, *28*, 146−156.
(98) Li, Z.; Liu, X.; Pei, Y.; Wang, J.; He, M. Design of Environmentally Friendly Ionic Liquid Aqueous Two-Phase Systems for the Efficient and High Activity Extraction of Proteins. *Green Chem.* **2012**, *14*, 2941−2950.